Acta of Bioengineering and Biomechanics
Vol. 19, No. 2, 2017

Original paper
DOI: 10.5277/ABB-00510-2015-04

Structure and corrosion resistance of Co-Cr-Mo alloy used in Birmingham Hip Resurfacing system

EWA DOBRUCHOWSKA*, MONIKA PAZIEWSKA, KRZYSZTOF PRZYBYL, KAZIMIERZ RESZKA

Koszalin University of Technology, Faculty of Technology and Education, Koszalin, Poland.

Purpose: The endoprostheses made of cobalt-chromium-molybdenum (Co-Cr-Mo) alloys belong to the group of the most popular metallic implants used for reconstruction of hip joints. For such biomaterials, the primary goal is a correct and long-term functioning in the aggressive environment of body fluids. Therefore, the purpose of this study was to examine both the morphology and the corrosion resistance of implants made of the cobalt alloy used in Birmingham Hip Resurfacing (BHR) system (Smith & Nephew). For comparative purposes, the electrochemical studies were done for the nitrided stainless steel – Orthinox. *Methods*: Observations of the microstructure of the material under investigation were performed by means of the optical metallographic microscope and the scanning electron microscope. Furthermore, Energy Dispersive X-ray Spectroscopy was used to analyse the chemical composition of the endoprosthesis. Characterisation and evaluation of electrochemical corrosion resistance of the selected alloys were performed by potentiodynamic polarisation tests. *Results*: The structural studies confirmed that Co-Cr-Mo (BHR system) is characterised by a typical dendritic microstructure with carbide precipitates, mainly $M_{23}C_6$, within the interdendritic areas. The results of the polarisation measurements showed that the cobalt alloy investigated exhibits lower corrosion potential than Orthinox in the utilised environments (3% NaCl, simulated body fluid – Hank's Body Fluid). *Conclusions*: However, the high passivation ability of the Co-Cr-Mo alloy, as well as its resistance to the initiation and propagation of localised corrosion processes, indicate that this material is significantly more appropriate for long-term implants.

Key words: *cobalt-chromium-molybdenum alloy, Birmingham Hip Resurfacing, carbide precipitation, corrosion resistance, potentiodynamic polarisation, nitrided stainless steel*

1. Introduction

On the basis of arthroplasty statistics, an upward trend in the frequency of implemented surgeries, where disease-affected joint is replaced by its artificial counterpart, is clearly distinct [1], [9], [10]. With an increasing availability of the latter, it is essential that possible complications due to the placement of a foreign matter inside the human body be taken into account. The local tissue response against the presence of metallic implant may be caused by corrosion developing on the implant surface. The corrosion process is mediated mainly by a damage of an implant protective layer or by migration of ions through the layer. Released ions and insoluble products of material degradation, from a few nanometres to a few millimetres in size, accumulate in the space between the implant and the bone, deepening the damage to endoprosthesis. Nickel, iron, aluminium, chromium or vanadium ions can accumulate in the soft tissues surrounding the joint, where they become targets for immune cells (particularly macrophages) of the recipient organism and cause extensive inflammatory reaction. Further, they can accumulate in the lymph nodes or, with the blood, migrate throughout the whole organism. Their activity often happens to be toxic, and consequently, can lead to dangerous health complications such as synovitis, bleeding, gout, nephropathy, cancer and, ultimately, the patient's death [4], [16], [17], [25].

The type and intensity of corrosion that develops during the contact of metallic biomaterial with body fluids depend on the geometrical characteristics of the

* Corresponding author: Ewa Dobruchowska, Koszalin University of Technology, ul. Śniadeckich 2, 75-453 Koszalin, Poland. Tel: +48 94 348 66 51, e-mail: ewa.dobruchowska@tu.koszalin.pl

Received: November 9th, 2015
Accepted for publication: July 5th, 2016

implant, its chemical and phase composition, the load type and its distribution and the implant mobility. On areas of an implant not subjected to a load, the prevailing type of corrosion is pitting. Depending on the implant residence time in a biological environment, besides of the typical corrosion pits, damage characteristic of crevice corrosion and fretting occurs, especially on the contact surfaces of cooperating parts [4], [6], [7], [16], [17].

To extend the proper functioning of the prosthesis in the environment of tissues and body fluids, new technological solutions are being searched for, with particular attention to the selection of appropriate materials. Modern materials such as cobalt-chromium (or cobalt-chromium-molybdenum) alloys replace the older versions like austenitic stainless steels. The fundamental criterion in selecting of material for biomedical purposes is biotolerance. Subsequently, one should pay attention to corrosion resistance, fine grain structure, distribution uniformity of elements and precipitates, mechanical properties (low Young's modulus, abrasion resistance, ability to suppress the vibration) and cost-effective production, exploitation and repair [3], [4], [7]. Therefore, conducting systematic research, analysing structural properties of materials and their susceptibility to the propagation of corrosion processes is a key factor in proper selection of alloying metals for the long-term endoprosthesis.

The purpose of this study was to examine the morphology and to identify the specific structural properties of implants made of the Co-Cr-Mo alloy used in BHR system. Furthermore, the corrosion resistance of Co-Cr-Mo was evaluated. In general, Co-Cr-Mo alloys are known to possess both high mechanical strength and corrosion resistance, the latter being mainly due to high ability to the surface passivation. However, it was found that implants made of cobalt-chromium-molybdenum alloys may release metal ions (Co, Cr, and Mo, respectively) into surrounding tissues. The reason for such behaviour is dissolution and/or breakdown of a surface oxide layer. The phenomenon has complex nature and is largely dependent on the alloy composition and the composition of the corrosive medium [21]. Corrosion studies conducted in various biological fluids by Hsu et al. can serve as an example. They demonstrated that Co-Cr-Mo alloys (60–64 wt.% of Co, 27–30 wt.% of Cr, 5–7 wt.% of Mo, and Ni < 1%, Mg < 1%, Fe < 1%) exhibit relatively narrow passive region when measured in serum and joint fluid, and a much broader one when tested in an urine environment [12]. In the present work, the corrosion behaviour of Co-Cr-Mo (used in BHR system) was checked in sodium chloride solution and simulated body fluid (Hank's Body Fluid). For comparative purposes, the electrochemical tests were also made for nitrided stainless steel – Orthinox. Both materials are currently used in orthopaedic surgeries as hip joint endoprostheses with increasing tendency to exclude the nitrided stainless steel.

2. Materials and methods

2.1. Materials

Within this work, the hip joint endoprosthesis made of Co-Cr-Mo cast alloy (Smith & Nephew, Great Britain) has been tested. The Co-Cr-Mo alloy is a modification of the classical Vitallium (the composition by weight: 62.50% Co, 30.80% Cr, 5.10% Mo, 0.50% Mn, 0.40% C, 0.30% Si, 0.40% Fe) and it is associated with the arthroplasty technique known as Birmingham Hip Resurfacing. The exact chemical composition of the alloy is protected by the company and is not accessible to the user. The hip joint endoprosthesis manufactured by Smith & Nephew is dedicated to young patients, exhibiting significant physical activity [13].

The nitrided stainless steel Orthinox produced by Stryker Howmedica Osteonics, USA (the composition by weight: 0.03% C, 4.00% Mn, 9.00% Ni, 20.50% Cr, 2.20% Mo, 0.40% N, 0.30% Nb, Fe – balance) is an austenitic stainless steel of a relatively high nitrogen content, which is a modification of 316 LVM steel. The implant, according to the literature data, is intended for medium- and long-term use [18].

2.2. Structural studies

Observations of the microstructure of the material under investigation (Co-Cr-Mo, Smith & Nephew) were performed by means of the optical metallographic microscope (MM) Nikon MA-200 and the scanning electron microscope (SEM) LV 5500 (JEOL Company) equipped with X-ray microanalyser (Oxford Instruments). MM images were recorded with DS-FI1 digital camera and Nikon's NIS-Elements software. The observations with SEM were carried out in a vacuum environment at a pressure of 2×10^{-4} Pa. The voltage accelerating the electron beam (probe) of 20 kV was applied. Each obtained image, regardless of the technique used, was supplied with an adequate

scale bar. Furthermore, chemical composition of the endoprosthesis was also tested by the quantitative microanalysis using the Energy Dispersive X-ray Spectroscopy (EDX). The examination was conducted on the metallographic cross-sections of the specimens. The samples were obtained by mechanical grinding with abrasive papers of various grit, and subsequent mechanical polishing by means of polishing canvas and a slurry of alumina. Then, as-prepared metallographic specimens were chemically etched by immersion in a mixture of concentrated hydrochloric acid and nitric acid (3:1). Additionally, corroded parts of the implant surface were observed with SEM. In this case, the samples were not treated in any way so as not to damage the original structure, instead, they were washed in ethanol by using an ultrasonic bath.

2.3. Electrochemical studies

Characterisation and evaluation of electrochemical corrosion resistance of selected alloys (Co-Cr-Mo, Smith & Nephew; Orthinox, Stryker Howmedica Osteonics) were performed by means of potentiodynamic polarisation tests, during which the polarisation curves were recorded using Atlas 9833 potentiostat (Atlas Sollich, Poland). The measurements were carried out in a conventional three-electrode electrolytic cell in an environment of simulated body fluid – Hank's Body Fluid and 3 wt.% NaCl solution, at room temperature (25 ± 1 °C). The reference electrode was a saturated calomel electrode (SCE, $Hg/Hg_2Cl_2/KCl$), and as the auxiliary electrode (counter electrode), a platinum plate was used. An active surface of the samples (working electrodes) each time had 0.3 cm^2. Prior to the beginning of the polarisation tests, the samples were kept in contact with the corrosive medium for 1 h at the open circuit conditions. The measurements were carried out at the scan rate of 0.001 V/s. The tests were repeated at least three times for each sample until obtaining similar polarisation curves. The curves were subsequently used to determine the corrosion process parameters, i.e., the corrosion potential (E_{corr}) and the corrosion current density (i_{corr}), by the Tafel extrapolation method [19]. The polarisation resistance (R_p) values were calculated from the Stern–Gaery equation. The tests were made on the surface and on the cross-section of each endoprosthesis. A series of cyclic tests was also performed in order to confirm the stability of the passive layer formed on the surface of selected materials.

3. Results

3.1. Morphology and chemical composition

The structural study of the metallographic cross-sections of the Co-Cr-Mo alloy specimens was mainly focused on characterisation of precipitates typical of this biomaterial. The structure of the alloy under investigation, imaged by the optical metallographic microscope, is shown in Fig. 1. The Co-Cr-Mo alloy has a morphology similar to an inhomogeneous austenite which demonstrates a distinct chemical segregation. The alloy is characterised by a typical dendritic microstructure with precipitates within the interdendritic areas. The structure of a typical precipitate present in the Co-Cr-Mo (BHR) is shown in Fig. 2. It exhibits the shape that can be described as intermediate between the lamellar structure and the star-like structure and possesses characteristicly notched surface.

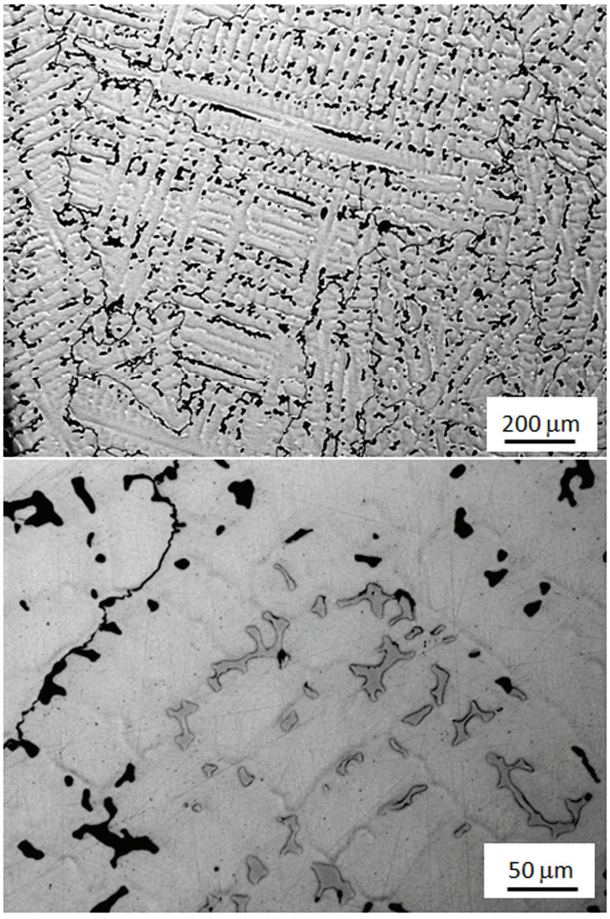

Fig. 1. Structure of Co-Cr-Mo alloy used in Birmingham Hip Resurfacing system – images obtained with optical metallographic microscope

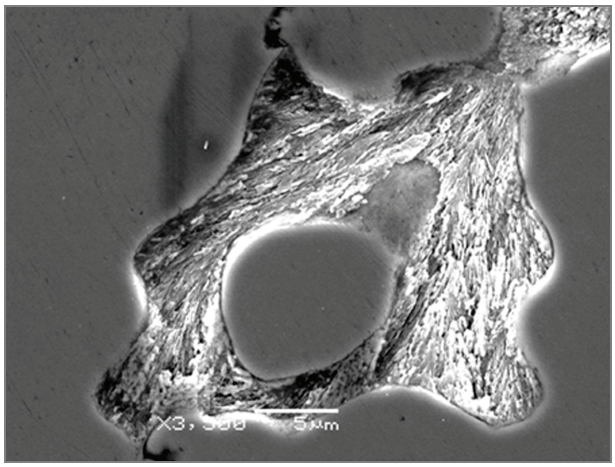

Fig. 2. Structure of typical carbide precipitate occurring in Co-Cr-Mo alloy used in Birmingham Hip Resurfacing system – image obtained with scanning electron microscope

Table 1. Results of EDX microanalysis obtained for Co-Cr-Mo alloy matrix and carbide precipitates

Element	Metallic alloy matrix wt. %*		Carbide precipitate wt. %*		Carbide precipitate wt. %	
	(1)	(2)	(1)	(2)	(1)	(2)
C	6.00	6.00	6.00	6.00	15.24	12.87
Co	59.56	58.09	16.25	23.72	14.65	21.99
Cr	28.19	28.71	62.25	55.44	56.13	51.39
Mo	5.51	6.23	15.49	14.83	13.97	13.75
Si	0.73	0.97	–	–	–	–

* Values calculated after correction for the carbon contribution.

Table 1 summarises the results of EDX microanalysis of two types of areas: metallic matrix of Co-Cr-Mo alloy and precipitates. The table shows the results of two selected measurements taken for each of the areas. The values included in the table are expressed in % by weight and they correspond to the mutual proportions between the different elements. In all the cases a significant contribution of carbon was observed. However, it should be noted that carbon may appear due to contamination of the compounds from the vacuum environment (a vacuum is generated with the use of the oil pump) and as the carbon compounds desorbed from the surface of the working chamber of the microscope. In this regard, Table 1 shows the composition of the analysed areas corrected for the contribution of carbon. It was assumed that the weight fraction of carbon in the measurement environment should not exceed 6%. In the case of precipitates, not corrected results are also presented. Nevertheless, in both cases, the results should be treated not as absolute values but as an indication of the relative proportions between various metallic components of the alloy.

The chemical composition analysis of the precipitates and the Co-Cr-Mo metallic matrix has shown that the precipitates are significantly enriched in molybdenum and strongly depleted of cobalt as compared to the matrix. Additionally, in their case, the chromium contribution is much higher than that of cobalt, unlike in the metallic alloy.

3.2. Corrosion resistance

The electrochemical tests were performed for the metal hip replacement made of Co-Cr-Mo alloy (BHR, Smith & Nephew) and nitrided stainless steel – Orthinox (Stryker Howmedica Osteonics). Studies of the outer surface of both implants which comes into direct contact with the patient's body were carried out in Hank's Body Fluid. In order to characterise the materials and compare the properties of the surface and the core of each endoprosthesis independently, a series of tests were performed using 3 wt.% NaCl solution (Fig. 3).

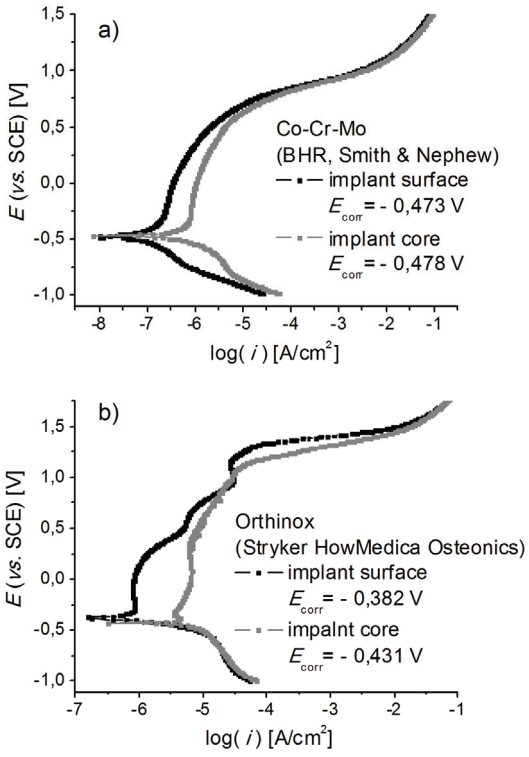

Fig. 3. Polarisation curves obtained for Co-Cr-Mo (BHR, Smith & Nephew) (a) and Orthinox (Stryker Howmedica Osteonics) (b) implants in 3 wt.% NaCl solution

Example polarisation curves, shown in Fig. 3a, obtained for the surface and the core of the Co-Cr-Mo implant have a similar shape for both the cathodic (up to the value of the corrosion potential) and the anodic (above E_{corr}) branches. The corrosion potentials assume similar values in both cases and amount to –0.473 V and –0.478 V for the outer surface and for the core of the implant, respectively. Subsequently, above the potential of ca. –0.360 V, a significant decrease in the rate of the anodic current density rise is observed that indicates the setting of passivation process (the formation of a thin layer of insoluble products of anodic reactions, e.g., oxides) inhibiting the corrosion process. The above-mentioned properties show that both test samples (the surface and the core), and thus the implant as a whole, are characterised by similar corrosion susceptibility and passivation ability in a given measurement environment. On the other hand, the corrosion current density (the quantity directly proportional to the speed of the corrosion process) determined for the core of the implant (i_{corr} = 0.23 × 10^{-6} A/cm^2) is higher than that obtained for its surface (i_{corr} = 0.08 × 10^{-6} A/cm^2). This difference can be associated with a slightly higher roughness of the core sample (prepared as part of this work) in comparison with a highly polished outer surface of the implant. It is known that increased roughness favours development of corrosion changes, particularly in an environment rich in chloride ions, facilitating the adhesion of ions and their mechanical anchoring.

Polarisation curves obtained for Orthinox in 3 wt.% NaCl solution (Fig. 3b) are characterised by a similar course only in the cathodic range. The corrosion potentials, determined for both samples are slightly different and take the values of –0.382 V and –0.431 V for the outer surface and for the core of the implant, respectively. In contrast to the cathodic branches of the corrosion characteristics, differences in the shape of anodic ones are strongly pronounced. Disparities are particularly evident within a passive region, which is easier to achieve in the case of the sample exposing the nitrided surface. After crossing the passivation potential E_{pp} = –0.305 V, there is a clear drop in the anodic current density visible here. Besides, characteristic inflexions of the polarisation curve are observed, which could be attributed to the transpassive dissolution of nitrides produced from the steel components in the nitriding process. In particular, the peak located at ca. 0.900 V is assigned to Cr_2N oxidation [14]. The polarisation curve recorded for the core is devoid of the characteristic transitions associated with the metal nitrides oxidation. Yet, it is characterised by higher values of the current density. The corrosion current density is equal to 5.13 × 10^{-6} A/cm^2, while for the outer surface of the implant i_{corr} = 1.00 × 10^{-6} A/cm^2. This suggests that corrosion changes occur faster within the core than at the nitrided surface of the implant. However, due to considerable disproportions in the course of the cathodic and anodic branches of the polarisation curves obtained, the i_{corr} values determined should be treated in an approximate way.

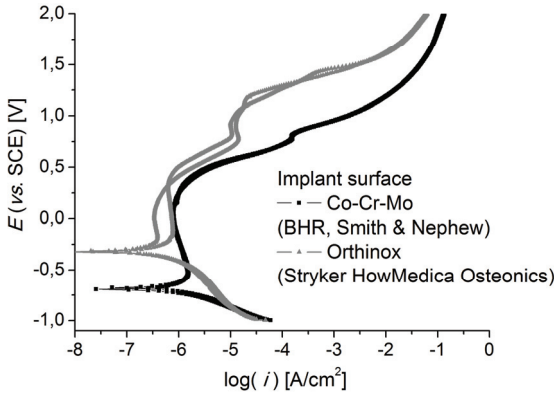

Fig. 4. Polarisation curves obtained for the surfaces of Co-Cr-Mo (BHR, Smith & Nephew) and Orthinox (Stryker Howmedica Osteonics) implants in Hank's Body Fluid

Figure 4 shows a comparison of potentiodynamic characteristics obtained for surfaces of both implants tested in the simulated body fluid – Hank's Body Fluid. On the graph, two polarisation curves obtained for each sample have been set together in order to confirm reproducibility of the results. The parameters characterising the corrosion process are summarised in Table 2. In addition to i_{corr} and E_{corr}, the table contains values of polarisation resistance (R_p). According to the Stern –Geary equation, R_p, is inversely proportional to the current density at the corrosion potential, and similarly to i_{corr}, may be regarded as a measure of the corrosion rate [24]. Based on the data presented, one can concluded that Co-Cr-Mo (BHR) shows much lower E_{corr} in comparison with Orthinox in the corrosive environment used. On the other hand, the values of i_{corr} and R_p do not differ greatly from those determined for the nitrided stainless steel. In both cases, initiated anode reactions lead to formation of resistive (passive) layers on the implant surfaces. The passive region ends when the sample surface achieves the breakdown potential (E_b). E_b corresponds to the potential beyond which the value of the current density increases rapidly [5] pointing to the breakdown of the passive layer and further metal oxidation or dissolution of the passive layer. On the basis of the corrosion characteristics shown in Fig. 4 one can determine the "widths" of the passive regions (ΔE_p) which extend from –0.210 V up to 0.352 V

for Orthinox and from –0.590 V up to 0.360 V for Co-Cr-Mo (BHR), respectively. The ΔE_p value for the cobalt alloy is thus 0.950 V.

Table 2. Statement of the average (of three measurements) parameters characterising the corrosion processes occurring onto the surface of implants investigated in Hank's Body Fluid

Corrosion process parameters	Co-Cr-Mo (BHR, Smith & Nephew)	Orthinox (Stryker HowMedica Osteonics)
E_{corr} [V]	–0.663 ± 0.006	–0.300 ± 0.031
i_{corr} [A/cm^2]	$1.00 \times 10^{-6} \pm 0.13 \times 10^{-6}$	$0.70 \times 10^{-6} \pm 0.08 \times 10^{-6}$
R_p [Ωcm^2]	42 240 ± 5 491	69 769 ± 7 326

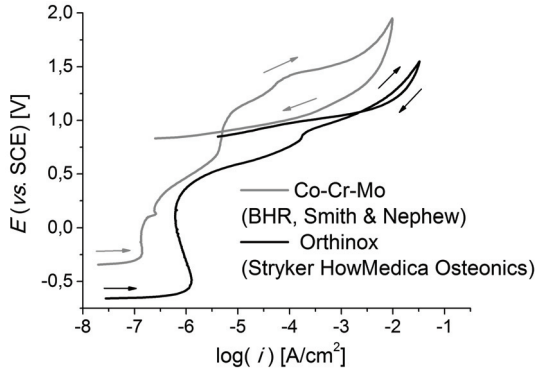

Fig. 5. Cyclic anodic polarisation curves obtained for the surfaces of Co-Cr-Mo (BHR, Smith & Nephew) and Orthinox (Stryker Howmedica Osteonics) implants in Hank's Body Fluid

Figure 5 presents the results of cyclic polarisation measurements that were carried out in order to verify the localised corrosion susceptibility of the endoprostheses being tested. In the case of the implant made of Orthinox, the presence of a clear hysteresis loop is observed, which indicates the material susceptibility to this type of corrosion changes in the Hank's Body Fluid environment. Hysteresis is a consequence of the passive layer destruction due to formation of stable pits and their further growth [8]. In fact, the microscopic examination done after the cyclic polarisation measurements revealed the presence of numerous pits within the test area (Fig. 6a). The curve obtained, for the implant made of the cobalt alloy is similar in both directions. Additionally, no clear pits were noticed during the microscopic observation (Fig. 6b) done for areas exposed to the corrosive medium. The obtained curve, which is probably a result of uniform corrosion occurring in the transpassive region and/or oxygen evolution, is characteristic of alloys resistant to initiation and propagation of localised corrosion [2].

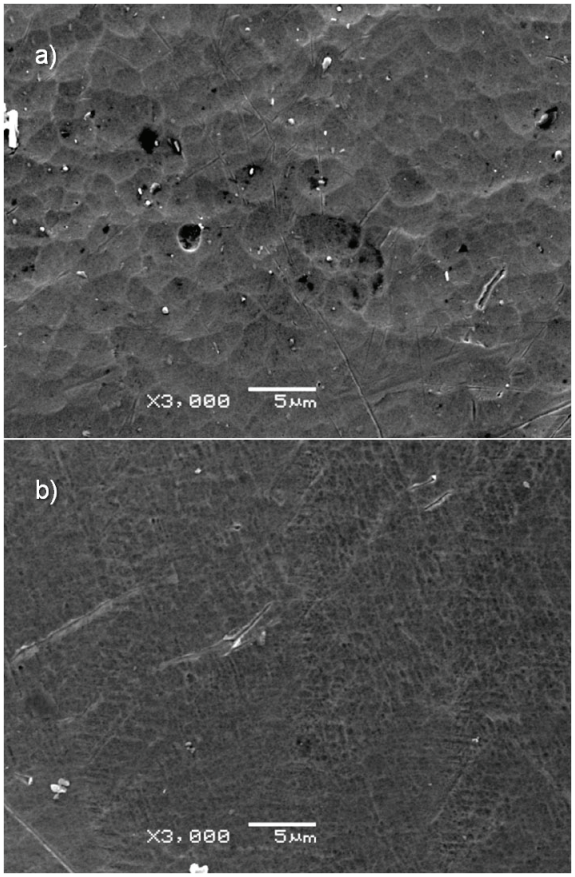

Fig. 6. SEM images of Orthinox surface (a) and Co-Cr-Mo (BHR, Smith & Nephew) surface (b) treated with Hank's Body Fluid

4. Discussion

The clinical success of implants made of cobalt-chromium alloys (including Co-Cr-Mo) is largely dependent on their microstructure which must resist mechanical stress of the musculoskeletal system and difficult biochemical conditions posed by fluids and tissues of the human body. As-cast Co-Cr alloys form microstructures with compact precipitates present in the metal matrix. Based on the literature reports, it should be assumed that they have a character of carbides [11], [20], [22]. Generally, the type of carbide precipitates and their morphology are dependent on the solubility of carbides in cobalt. Thus, depending on the chemical composition and processing conditions, differently structured carbides such as MC, M_3C_2, M_6C, M_7C_3 and $M_{23}C_6$ may appear in the metallic matrix of cobalt alloys. However, in the case of

as-cast cobalt-chromium alloys, M_6C, M_7C_3 and $M_{23}C_6$ carbides are the most common [23]. Precipitates of shapes similar to those observed in the Co-Cr-Mo alloy (BHR) under study have been described in the work of Narushima et al. [22]. They were identified as $M_{23}C_6$ type carbides, and the authors suggested that the primary metal included in their composition is chromium. This is consistent with the results of the chemical analysis performed for precipitates present in the alloy under investigation. It should also be noted that the carbides can be converted during the heat treatment (at ca. 1200 °C, in this case) and the subsequent cooling. In higher temperature range, the precipitation of M_6C prevails, and in the range of lower temperatures – the isolation of $M_{23}C_6$. Conversion of $M_{23}C_6$ type carbides in the M_6C is associated with greater stability of M_6C carbide at temperatures ranging from 1165 °C to 1230 °C. The $M_{23}C_6$-M_6C-$M_{23}C_6$ transformation is accompanied by a pronounced increase in the chromium concentration within the interdendritic areas [20]. Both observations described above and the results of the studies performed support the conclusion that $M_{23}C_6$ is a dominant carbide present in the Co-Cr-Mo alloy, used by Smith & Nephew in the BHR system.

Carbide phase is much harder than the metallic alloy matrix, and its presence reduces the intensity of the process of material consumption. On the other hand, the carbide precipitates also promote nucleation of microcracks within their volume and at the carbide–matrix borders. This leads to a significant reduction in ductility, impact strength and cracking resistance of alloys, particularly when carbides are present in the form of continuous films at the grain boundaries (also presented in this work in Fig. 1) [20], [23]. Besides, formation of carbides of alloying elements (mainly Cr) causes that the metallic matrix is depleted of chromium in the vicinity of the precipitates [15]. All the described effects above may adversely affect corrosion resistance of as-cast cobalt alloys increasing their susceptibility to localised corrosion. Therefore, one of the main objectives of this work was to carry out the electrochemical tests in order to determine the corrosion resistance of the metal hip replacement made of Co-Cr-Mo alloy (BHR, Smith & Nephew) as well as to compare it to the corrosion resistance of the older generation prosthesis, made of nitrided stainless steel – Orthinox (Stryker Howmedica Osteonics).

Studies performed in two different environments (Hank's Body Fluid and 3 wt.% NaCl solution) showed that Co-Cr-Mo (BHR) exhibits greater susceptibility to corrosion (lower E_{corr}) than Orthinox. On the other hand, similar corrosion resistance (in 3 wt.% NaCl) of the core and surface of the implant made of the cobalt alloy indicates that both samples underwent oxidation in the air resulting in the formation of a natural thin passive film. The passive layer, created spontaneously on the surface of such alloys, contains primarily Cr_2O_3 and, in minor amounts, cobalt and molybdenum oxides [12], [21]. Due to the presence of the oxide layer, both samples of the Co-Cr-Mo alloy under study achieve passivity without passing through the active –passive transition, and the passive range is set directly after the Tafel region. The stainless steel behaves alternatively. In this case, the transition to the passive state involves the achievement of a current maximum placed at the critical passivation potential. It should be noted here that a slightly lower corrosion potential estimated for the implant core (and the higher value of the corrosion current density) relative to the implant surface is caused by steel nitriding [14].

The differences between the corrosion potential values determined for both implants are particularly evident for tests carried out in Hank's Body Fluid. It is assumed that the stronger the natural oxide layer on the Co-Cr-Mo alloy, the better the corrosion resistance and the less intense the release of the metal ions from the implant [12]. Thus, the presence of areas depleted of chromium in the vicinity of the precipitates can promote early corrosion changes observed. Co-Cr-Mo (BHR), however, exhibits more stable passive region compared to Orthinox that extends over a wide potential range. This may be the caused by an increase in the thickness of the passive layer occurring during the experiment of electrochemical corrosion. According to the literature data, until the potential of 0.300 V is achieved (in Hank's Body Fluid, vs. SCE, for the alloy of similar composition), the passive layer dominated by Cr_2O_3 and $Cr(OH)_3$ increases along with the potential at a rate of ca. 1.5 nm/V. Using the X-ray photoelectron spectroscopy, it was demonstrated that the thickness of the layer formed by these compounds at the potential equal to 0.300 V reaches 3.1 nm. At more positive potentials, significant changes in the layer thickness and composition occur – Co and Mo oxides are incorporated into the layer structure. These changes are accompanied with an increase in the current density, slow at first and then rapid which is tantamount to breaking the passive state [21]. These observations are fully consistent with the results of potentiodynamic polarisation tests carried out within this work.

The cyclic polarisation measurements performed confirm the possibility of the formation and growth of the passive layer in the environment of Hank's Body

Fluid. The increase of the layer thickness and changes in its composition, caused by oxides incorporation into the material surface, suppress the development of pitting corrosion process [17]. This is evidenced by high ability of the Co-Cr-Mo (BHR) to pits repassivation – characteristic of materials exhibiting resistance to the propagation of localised corrosion [2]. Thus, the presence of carbides (mainly chromium ones) does not seem to increase the susceptibility of Co-Cr-Mo (BHR) considerably to this type of corrosion, even though they may contribute to the generation of microcracks, and their formation may lead to a local depletion of chromium in the vicinity of the precipitates.

5. Conclusions

In conclusion, the research performed for Co-Cr-Mo alloy used by Smith & Nephew in the BHR system indicated that it is characterised by a typical dendritic microstructure with carbide precipitates within interdendritic areas. The precipitates are significantly abundant in chromium and molybdenum and simultaneously poorer in cobalt compared to the metal matrix of the alloy. Further, the shape and the chemical composition of precipitates suggest that $M_{23}C_6$ is the dominant form of carbides present in the material investigated.

The electrochemical studies performed for Co-Cr-Mo alloy, in comparison to Orthinox, indicated that it exhibits lower corrosion potential, and then greater corrosion susceptibility in the environments utilised (3 wt.% NaCl, simulated body fluid – Hank's Body Fluid) than the nitrided stainless steel. On the other hand, Co-Cr-Mo demonstrates high passivation ability within both areas tested– the external surface and the core of the implant. Furthermore, it is characterised by high resistance to the initiation and propagation of localised corrosion processes (in spite of the presence of numerous carbide precipitates). Taking into account that prevailing type of corrosion on the implant areas not subjected to a load is pitting, these features make Co-Cr-Mo (BHR) alloy more suitable for the production of endoprostheses intended for the long-term use than the nitrided stainless steel.

References

[1] *Annual Report on Hip and Knee Arthroplasty Data*, AJRR Annual Report 2013, Rosemont, IL, 2014.

[2] ASTM G61-86, *Standard Test Method for Conducting Cyclic Potentiodynamic Polarization Measurements for Localized Corrosion Susceptibility of Iron-, Nickel-, or Cobalt--Based Alloys*.

[3] BAHRAMINASAB M., SAHARI B.B., EDWARDS K.L., FARAHMAND F., ARUMUGAMG M., HONG T.S., *Aseptic loosening of femoral components – A review of current and future trend in materials used*, Materials and Design, 2012, 42, 459–470.

[4] BRONZINO J.D., *The Biomedical Engineering Handbook*, 2nd ed., CRC Press LLC, 2000.

[5] CHOHAYEB A.A., FRAKER A.C., EICHMILLER F.C., WATERSTRAT R., BOYD J., *Corrosion behaviour of dental casting alloys coupled with titanium*, [in:] S.A. Brown, J.E. Lemons (eds.), *Medical application of titanium and its alloys: the material and biological issues*, ASTM, Conshohocken 1996.

[6] COOPER J.H., DELLA VALLE C.J., BERGER R.A., TETREAULT M., PAPROSKY W.G., SPORER S.M., JACOBS J.J., *Corrosion at the head-neck taper as a cause for adverse local tissue reactions after total hip arthroplasty*, J. Bone Joint Surg. Am., 2012, 94(18), 1655–1661.

[7] COOPER J.H., URBAN R.M., WIXSON R.L., MENEGHINI R.M., JACOBS J.J., *Adverse local tissue reaction arising from corrosion at the nemoral neck-body junction in a dual-taper stem with a cobalt-chromium modular neck*, J. Bone Joint Surg. Am., 2013, 95(10), 865–872.

[8] GALVELE J.R., *Tafel's law in pitting corrosion and crevice corrosion susceptibility*, Corros. Sci., 2005, 47, 3053–3067.

[9] GARELLICK G., KARRHOLM J., LINDAHL H., MALCHAU H., ROGMARK C., ROLFSON O., *Swedish Hip Arthroplasty Register*, Annual Report 2013, Gothenburg, 2014.

[10] GRAVES S., *Hip and knee arthroplasty*, AOAJRR Annual Report 2013, Adelaide 2013.

[11] HERNANDEZ-RODRIGUEZ M.A.L., MERCADO-SOLIS R.D., PEREZ--UNZUETA A.J., MARTINEZ-DELGADO D.I., CANTU-SIFUENTES M., *Wear of cast metal–metal pairs for total replacement hip prostheses*, Wear, 2005, 259, 958–963.

[12] HSU WEN-WEI R., YANG CH., HUANG CH., CHEN Y., *Electrochemical corrosion studies on Co-Cr-Mo implant alloy in biological solutions*, Mater. Chem. Phys., 2005, 93, 531–538.

[13] http://www.smith-nephew.pl/. Accessed 11.09.2015.

[14] JAGIELSKA-WIADEREK K., BALA H., WIECZOREK P., RUDNICKI J., *Depth characterization of glow-discharge nitrided layer produced on AISI 4140 steel*, Arch. Metall. Mater., 2010, 55, 515–519.

[15] JIAO S.Y., ZHANG M.C., ZHENG L., DONG J.X., *Investigation of Carbide Precipitation Process and Chromium Depletion during Thermal Treatment of Alloy 690*, Metall. Mater. Trans. A, 2010, 41A, 26–42.

[16] KIEL M., KRAUZE A., MARCINIAK J., *Corrosion resistance of metallic implants used in bone surgery*, Arch. Mat. Sci. Eng., 2008, 20, 77–80.

[17] KIEL-JAMROZIK M., SZEWCZENKO J., BASIAGA M., NOWIŃSKA K., *Technological capabilities of surface layers formation on implant made of T-6Al-4V ELI alloy*, Acta of Bioengineering and Biomechanics, 2015, 17–1, 31–37.

[18] LEWTHWAITE S.C., SQUIRES B., GIE G.A., TIMPERLEY A.J., PHIL D., LING R.S.M., *The Exeter™ Universal Hip in Patients 50 Years or Younger at 10–17 Years' Followup*, Clin. Orthop. Relat. R., 2008, 466, 324–331.

[19] McCafferty E., *Validation of corrosion rates measured by the Tafel extrapolation method*, Corros. Sci., 2005, 47, 3202–3215.
[20] McMinn D.J., *Development of Metal/Metal Hip Resurfacing*, Hip. Int., 2003, 13(1), 41–53.
[21] Milosev I., *CoCrMo Alloy for Biomedical Applications*, [in:] S.S. Diokic (ed.), *Biomedical Applications*, Springer Science+Business Media, New York 2012.
[22] Narushima T., Mineta S., Kurihara Y., Ueda K., *Precipitates in Biomedical Co-Cr alloys*, JOM – J. Min. Met. Mat. S., 2013, 65, 489–503.
[23] Shi L., Northwood D.O., Cao Z., *The properties of a wrought biomedical cobalt-chrome alloy*, J. Mater. Sci., 1994, 29, 1233–1238.
[24] Stern M., Geary A.L., *Electrochemical polarization I. A Theoretical analysis of the Shape of polarization curves*, J. Electrochem. Soc., 1957, 104, 56–63.
[25] Thakur R.R., Ast M.P., McGraw M., Bostrom M.P., Rodriguez J.A., Parks M.L., *Severe persistent synovitis after cobalt-chromium total knee arthroplasty requiring revision*, Orthopedics, 2013, 36(4), e520–e524.